Motion of Submicron Particles in Supersonic Laminar Boundary Layers

Xing Li* and Bofeng Bai†
State Key Laboratory of Multiphase Flow in Power Engineering, Xi'an Jiaotong University, 710049 Xi'an, Shaanxi, People's Republic of China

DOI: 10.2514/1.J053364

Submicron-particle motion in laminar boundary layers is present in many practical applications. Some important findings on this issue have been achieved during the last decades, but many mechanisms in this process still remain unclear. In the present work, a model has been developed to describe the motion of the submicron particles in supersonic laminar boundary layers above an adiabatic plate along with the mainstream. In this model, the Lagrangian method is used to track the particles and calculate their trajectories, and the Eulerian method to calculate the flowfield. The effects of the entering position, Mach number, and the size and density of the particles were investigated. It is concluded that there are three particle-motion patterns when they enter the supersonic boundary layer, which are departure pattern, equilibrium pattern, and deposition pattern. The drag force and Saffman lift force were discovered to play dominating roles in deciding the patterns, and thermophoretic force and Brownian force are of less importance. A dimensionless number to describe these three patterns is suggested. This work was intended to provide an insight into the submicron-particle motion in the supersonic laminar boundary layer, which can be guidance for industrial applications involving this phenomenon.

Nomenclature

a	=	radius of particle, m
C_c	=	Stokes–Cunningham coefficient
C_D	=	drag coefficient
d_p	=	diameter of a particle, m
$\mathrm{d}t$	=	time step, s
$\mathrm{d}x$	=	spatial step, m
E_v	=	bulk modulus of fluid, Pa
F_B	=	Brownian force on a particle, N
F_D	=	drag force on a particle, N
F_S	=	Saffman lift force on a particle, N
F_T	=	thermophoretic force on a particle, N
f_T	=	dimensionless thermophoretic force
Kn	=	Knudsen number
Kn_0	=	initial Knudsen number
k_B	=	Boltzmann constant, $\mathrm{J} \cdot \mathrm{K}^{-1}$
Ma_p	=	particle Mach number
Ma_{p^0}	=	initial particle Mach number
m_p	=	mass of a particle, kg
R	=	gas constant, $\mathrm{J} \cdot \mathrm{kg}^{-1} \cdot \mathrm{K}^{-1}$
Re_p	=	particle Reynolds number
Re_{p^0}	=	initial particle Reynolds number
Stk	=	Stokes number
T	=	temperature of fluid, K
U	=	velocity of fluid, $\mathrm{m} \cdot \mathrm{s}^{-1}$
U_0	=	initial velocity of fluid, $\mathrm{m} \cdot \mathrm{s}^{-1}$
y_0	=	initial distance between the particle and the wall, m
y_{0e}	=	equilibrium initial position of the particle, m
ΔU	=	relative velocity between the particle and the fluid, $\mathrm{m} \cdot \mathrm{s}^{-1}$
δ_{ij}	=	Kronecker delta function
ζ_i	=	zero-mean unit-variance-independent Gaussian random number
λ_0	=	initial mean free path of a gas molecule, m
μ	=	dynamic viscosity of fluid, $\mathrm{Pa} \cdot \mathrm{s}$
μ_{g0}	=	initial dynamic viscosity of fluid, $\mathrm{Pa} \cdot \mathrm{s}$
ν	=	kinematic viscosity of fluid, $\mathrm{m}^2 \cdot \mathrm{s}$
ρ	=	density of fluid, $\mathrm{kg} \cdot \mathrm{m}^{-3}$
ρ_{g0}	=	initial density of fluid, $\mathrm{kg} \cdot \mathrm{m}^{-3}$
ρ_p	=	density of particle, $\mathrm{kg} \cdot \mathrm{m}^{-3}$
Φ	=	dimensionless number describing the particle-movement patterns

Received 25 January 2014; revision received 1 July 2014; accepted for publication 1 August 2014; published online 1 December 2014.

*Ph.D. Candidate; lx20032006@126.com.
†Professor; bfbai@mail.xjtu.edu.cn (Corresponding Author).

I. Introduction

THE submicron-particle motion in a supersonic laminar boundary layer is present in a wide range of applications. In gas turbines, ashes from the inadequately combusted fuel deposit on the turbine blades, and accumulate as the machine runs. In the deposition process, the ash particles move across the boundary layer before they reach the surface of the blade. The flow is generally transonic in the gas turbines. In this case, the knowledge of the motion of the ash particles in the high-speed laminar boundary layer is quite necessary. Another case is the droplets in the clouds that supersonic aircraft happen to fly into. These droplets flow across the boundary layer, and some deposit on the surface of the aircraft, probably resulting in the icing problem under the conditions of low temperature and high altitude, and seriously affecting the flight performance. In experimental investigations on the supersonic boundary layer, motion of tracer particles commonly occurs. Accurately predicting the motion properties of tracer particles is a key to the success of the experiments.

In the study of the motion of submicron particles in a boundary layer, the core problem is the deposition process of the particles on the wall. In a laminar boundary layer, particle deposition due to turbulent diffusion (i.e., turbulent deposition) does not occur. In many cases, the mechanism of the particle deposition is Brownian diffusion, and there exists a concentration boundary layer near the wall. But, in some cases, in which the wall is heated or cooled, the thermophoresis has to be taken into consideration. In the case in which the wall temperature is higher than the fluid temperature, the deposition is inhibited and the dust-free layer emerges. Particles seldom penetrate this layer and reach the wall. When the wall is cooled, the deposition is promoted. Under regular gravity, the gravitational deposition of the submicron particles can be neglected. It will be taken into account generally when the particle diameter is over 1.0 μm. In the presence of other external force fields, like electrical field [1], the deposition process caused by it has to be considered. In stagnation flows, the inertial deposition dominated by the Stokes number of the particles

can be significant. When $Stk \ll 1$, the inertial transport is negligible, whereas when $Stk > 1$, it is not negligible because of the relatively larger inertia of the particles.

Because of the wide application of thermophoresis, relevant researches have been found in great numbers, the majority of which are about the transport of small particles with thermophoresis in laminar boundary layers. Goren was the first to theoretically study the thermophoresis in laminar boundary-layer flows [2]. He investigated the flows on both hot and cold plates, and discovered the dust-free layer (or particle-free region) on heated objects. Mills et al. presented their findings concerning the deposition rate under the conditions of thermophoresis and wall suction in a laminar boundary layer of a flat plate [3]. Epstein et al. analyzed the thermophoretic transport of small particles in natural convection flow on a vertical plate under the conditions of both laminar and turbulent flows [4]. Gökog˘lu and Rosner systematically studied thermophoretically enhanced mass-transport rates on solid cold walls across the laminar as well as the turbulent boundary layers [5–7]. Garg and Jayaraj investigated the thermophoresis of aerosol particles over a cylinder and inclined plates [8,9]. Chiou and Cleaver, and Chiou published a series of papers on submicron-particle transport processes in laminar and turbulent boundary layers [10–13]. In general, most of the studies available adopted the analytical or Eulerian method to obtain the macroscopic parameters (e.g., deposition rate). However, some microscopic mechanisms remain unrevealed.

The purpose of this paper was to study the motion of the submicron particles when they enter the supersonic laminar boundary layer above an adiabatic plate along with the mainstream. In our work, we build a two-dimensional model to reveal the mechanisms in this process. We focus on the laminar boundary layer, excluding the situation when it turns into turbulent. First, we describe our research problem, and state the Eulerian–Lagrangian method and the force models. The force models are especially elaborated, followed by a grid-independent verification to ensure the accuracy of the modeling. Then, the role of each force is examined, and the reason why some particles move away from the wall is revealed. Next, the influencing factors, including the entering position, Mach number, and the size and density of particles, are investigated. In the following part, we present three particle-motion patterns and give a detailed analysis. Finally, we come up with a dimensionless number to describe these three motion patterns.

II. Problem Description

Our research problem can be simplified as the gas-particle flow above a flat plate, as shown in Fig. 1. Particles enter the domain above the plate at the speed of the main flow, which means there is no slip between the particles and the surrounding gas at the initial position. Then, some of the particles will enter the boundary layer, and some will not. Our work is focused on the particles entering the boundary layer. As the flow speed is high, the gas phase is regarded as compressible. For the dispersed phase, the particles are considered as spherical and monodispersed. As the size and volume fraction of the particles are small, their effect on the fluid and the particle–particle interaction are negligible. Among the forces exerted by the fluid on the particles, the drag force is the major one and has to be taken into consideration. In the supersonic boundary layer, the velocity and temperature gradients are large, and so the Saffman lift force and the thermophoretic force are also included. And, as the particles are submicron, Brownian motion is taken into account. As the density of the particles is very large compared with that of the gas, unsteady forces, including added mass force and Basset force, are neglected. According to the research of Bagchi and Balachandar [14], and Ling et al. [15], the net effects of unsteady forces are important when the particle-to-gas density ratio is small, and they decrease as the particle-to-gas ratio increases and the initial particle Reynolds number decreases. In our research, the particle-to-gas ratio is beyond 2500, and the particle Reynolds number is below 10 in most cases, and so the unsteady forces are neglected. In addition, the research of Tedeschi et al. also proves that the force model, only considering the quasi-steady force, is able to well predict the velocity of the particle after the oblique shock wave [16]. The Magnus force and gravitational force are also neglected for the condition considered in this problem. Because the characteristics of the particle motion are our main concern, the heat and mass transfer between the particles and the fluid is left out of our consideration. In addition, we focus on the particle movement in the fluid, not the particle–wall interaction, and so the reflection of the particles when they touch the wall is neglected, that is, we assume that the particles deposit on the wall once they reach it.

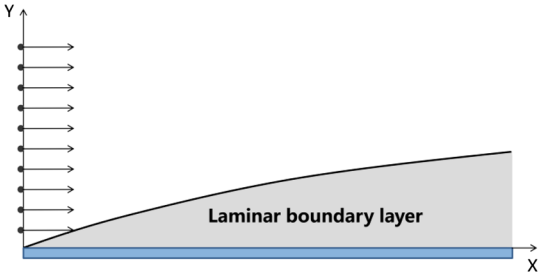

Fig. 1 Description of the problem.

III. Computational Model

A. Fluid-Force Models

The motion of each particle is expressed by Newton's second law of motion:

$$m_p \frac{\mathrm{d}^2 x}{\mathrm{d}t^2} = F_D + F_T + F_S + F_B \tag{1}$$

in which m_p is the particle mass, F_D is the drag force, F_T is the thermophoretic force, F_S is the Saffman lift force, and F_B is the Brownian force. The model of each force is carefully selected to accurately predict the trajectory of the particle.

1. Drag Force

The drag force of a spherical particle has been well studied for a very long time. Many effects should be considered when the particle is exposed to different surroundings. In our research, the particle Reynolds number, as well as the relative Mach number, is rather high, and the particles cannot change their velocities as fast as the fluid due to the inertia. And rarefaction may occur when the particles are submicron. For the flow condition of high relative Mach number, Henderson obtained a group of empirical expressions for all the flow conditions depending on the Mach number [17,18]. Tedeschi et al. proposed an expression valid for $Re_p < 200$, $Ma_p < 1$ from continuum to free molecular range [16], which agrees well with the experiment. Thus, we apply the expression proposed by Tedeschi et al. They introduced the correction coefficients for rarefaction and high Mach number, and the solution of k is also modified. The expression is as follows:

$$F = -6\pi\mu a k \Delta U[1 + 0.15(kRe_p)^{0.687}]\xi(Kn)C \tag{2}$$

or

$$C_D = \frac{24}{Re_p} k[1 + 0.15(kRe_p)^{0.687}]\xi(Kn)C \tag{3}$$

in which a is the radius of the particle, μ is the dynamic viscosity of the fluid, ΔU is the relative velocity between the particle and the fluid, $\xi(Kn)$ is the rarefied correction coefficient, and C is the correction coefficient for high relative Mach number. The expressions of $\xi(Kn)$ and C are

$$\xi(Kn) = 1.177 + 0.177\frac{0.851Kn^{1.16} - 1}{0.851Kn^{1.16} + 1} \tag{4}$$

and

$$C = 1 + \frac{Re_p^2}{Re_p^2 + 100} e^{-0.225/Ma_p^{2.5}} \tag{5}$$

In expressions (2) and (3), the coefficient k is the solution of the following equations:

$$a_1 k^{1.687} + a_2 k - 1 = 0 \tag{6}$$

$$a_1 = \frac{9}{4} 0.15 \frac{d_p}{a} \frac{Kn}{\varepsilon'} \left(\frac{2a}{d_p} \frac{S\sqrt{\pi}}{Kn} \right)^{0.687} \tag{7}$$

$$a_2 = 1 + \frac{9}{4} \frac{d_p}{a} \frac{Kn}{\varepsilon'} \tag{8}$$

in which d_p is the particle diameter, $S = U_0/\sqrt{2RT_\infty}$ is the molecular-speed ratio, $\varepsilon' = \frac{3}{8}(\sqrt{\pi}/S')(1 + S'^2)\mathrm{erf}(S') + e^{-S'^2}/4$, and $S' = (1 - k)S$.

2. Thermophoretic Force

In our study, the range of the Knudsen number is large. For the calculation of the thermophoretic force in the transition regime, Talbot et al. derived an interpolation formula that was widely used [19]. Their expression agrees within 20% or less with the data available in the entire range of Knudsen number. Later scholars like Sone and Aoki [20], Yamamoto and Ishihara [21], Loyalka [22], and Takata et al. [23] proposed more accurate solutions of the Boltzmann equation, among which Yamamoto and Ishihara solved the Boltzmann equation numerically and obtained good results. We take the solution proposed by Yamamoto and Ishihara as the calculating method of the thermophoretic force on a particle, for, in general, it agrees better with experimental results than the Talbot et al. expression, and is convenient to use. The dimensionless form of their solution is as follows:

$$f_T = \frac{16\pi}{5} \left[A_w H_o - A_o \left(H_w + \frac{5\sqrt{\pi}}{4} Kn\hat{k} \right) \right] \left(H_w + \frac{5\sqrt{\pi}}{4} Kn\hat{k} \right)^{-1} \tag{9}$$

in which A_w, A_o, H_w, and H_o are functions of the Knudsen number, and $\hat{k}$ is the ratio of thermal conductivity of the particle to that of the gas.

3. Saffman Lift Force

According to Saffman's theory, when a particle travels in the same direction with a shear flow, the flow velocity of the two sides of the particle in the direction perpendicular to the flow is not the same, resulting in a pressure difference on the two sides. Thus, a net force emerges in the direction perpendicular to the particle velocity (or fluid velocity), and is called lift force. When there is no velocity gradient or relative velocity between the particle and the fluid, the lift force disappears. In the cases of the particle lagging the fluid (the particle slower than the fluid) and the particle leading the fluid (the particle faster than the fluid), the directions of the lift force are opposite. The expression proposed by Saffman is

$$F_S = 6.46\mu a^2 \Delta U \left(\frac{1}{\nu} \frac{\mathrm{d}U}{\mathrm{d}y} \right)^{1/2} \tag{10}$$

in which ΔU is the particle slip velocity, ν is the fluid kinematic viscosity, and $\mathrm{d}U/\mathrm{d}y$ is the velocity gradient of the shear flow.

Some scholars, including Dandy and Dwyer [24], McLaughlin [25], Mei [26], Kurose and Komori [27], and Bagchi and Balachandar [28], worked out different forms of expressions afterward through theoretical or numerical methods. But, so far, Saffman's expression can meet the requirement of accuracy and is still widely used. Thus, in our work, we use his equation [Eq. (10)] to calculate the Saffman lift force.

4. Brownian Force

For submicron particles, Brownian motion cannot be neglected. The Brownian force can be modeled as a Gaussian white-noise random process with spectral intensity S_{ij}^n given by

$$S_{ij}^n = S_o \delta_{ij} \tag{11}$$

in which δ_{ij} is the Kronecker delta function, and

$$S_o = \frac{216\nu k_B T}{\pi^2 \rho d_p^5 (\frac{\rho_p}{\rho})^2 C_c} \tag{12}$$

Here, k_B is the Boltzmann constant, and C_c is the Stokes–Cunningham correction. The Brownian force is expressed as

$$F_{Bi} = \zeta_i \sqrt{\frac{\pi S_o}{\Delta t}} \tag{13}$$

in which ζ_i is the zero-mean unit-variance-independent Gaussian random numbers [29,30].

B. Flowfield Calculation

The flowfield in our study is supersonic and, thus, compressible. The equations for continuous phase include mass-conservation equation, momentum-conservation equation, and energy-conservation equation. The equation of state has to be taken into consideration also. As the gas does not meet the ideal-gas assumption, the *Redlich–Kwong* equation of state is applied. The effect of the particles on the fluid is negligible, and so in the gas-phase equations, there are no source terms.

The FLUENT code with a structured mesh is used to solve the two-dimensional flow governed by the compressible Navier–Stokes equations. The single-phase supersonic flowfield is calculated first, then the particles are injected into the flow and their trajectories are calculated with the flowfield. The fluid-force models are inserted through the user-defined function interface.

IV. Computational Parameters and Validation

A. Domain and Calculation Parameters

The simulation of submicron-particle dynamics is performed in a two-dimensional rectangular region with an adiabatic flat plate as the lower boundary. The length of the region in the y direction is set the same as that in the x direction to eliminate the effect of the upper bound on the flowfield. In this calculation, the computational domain is the region of $0 \le X \le 50$ mm, $0 \le Y \le 50$ mm. Particles are injected at a specific rate uniformly distributed along the inlet.

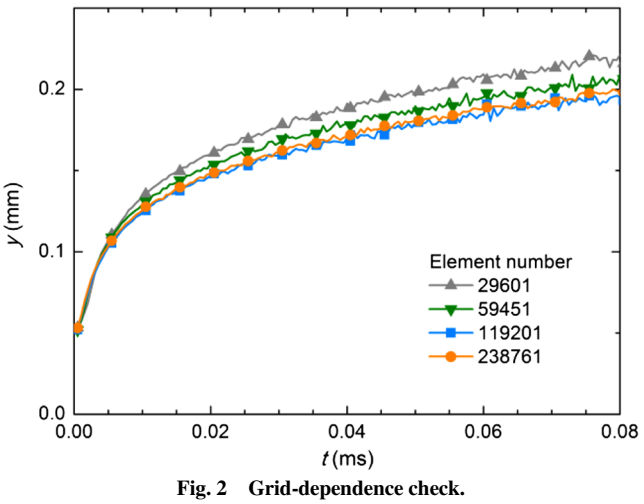

Fig. 2 Grid-dependence check.

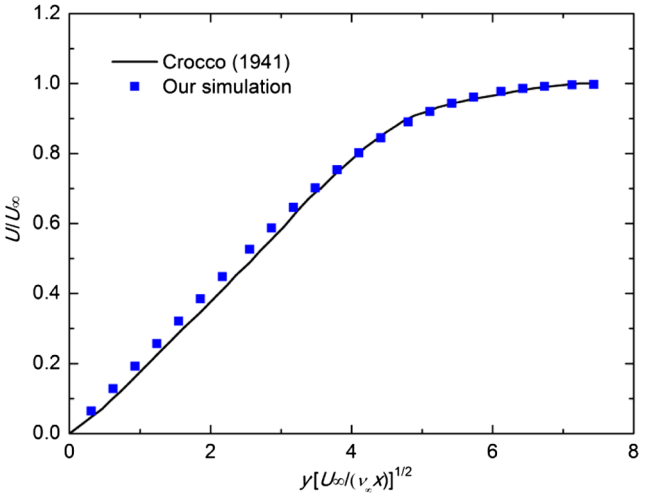

Fig. 3 Velocity distribution in the supersonic laminar boundary layer.

Influencing factors, including Mach number, particle diameter, and particle density, are examined. The Mach number ranges from 1.68 to 3.01, and the diameter of the submicron particles is from 0.05 to 1.0 μm. To investigate the effect of density, four kinds of particles with different densities are selected: carbon particle (2000 kg/m^3), water droplet (1000 kg/m^3), kerosene droplet (780 kg/m^3), and titanium dioxide particle (4000 kg/m^3). The gas is air. And the total pressure and total temperature of the inlet flow are 101 kPa and 421 K, respectively.

B. Validation

To eliminate the effect of the number of the mesh elements on the calculation, a grid-dependence check is operated. A comparison of particle y position with time by using meshes of different numbers is made to check the grid dependence. The particles are injected in the same y position. It is shown in Fig. 2 that the mesh with number exceeding 110,000 can satisfy the need to eliminate the effect of the grid. Thus, the mesh with 119,201 elements is used in the calculation.

So far, relevant experimental data on the motion of submicron particles in a supersonic boundary layer are not available. To validate the accuracy of our model, the simulating result of the velocity distribution in the supersonic laminar boundary layer above an adiabatic flat plate with the main flow of Mach 2.0 is compared with the analytical result proposed by Crocco [31]. Figure 3 shows that the simulating result is in good accordance with the analytical one.

V. Results

A. Role of Each Force

As we have mentioned previously, four forces are taken into consideration in our discussion. To know which force or forces play an important role, an investigation is made. The particles in Secs. V.A–V.D are all water drops. We have chosen four typical cases to examine the trajectories of the particles injected from the same initial position, as shown in Fig. 4. The four cases are with all forces, without Saffman lift force, without thermophoresis, and without

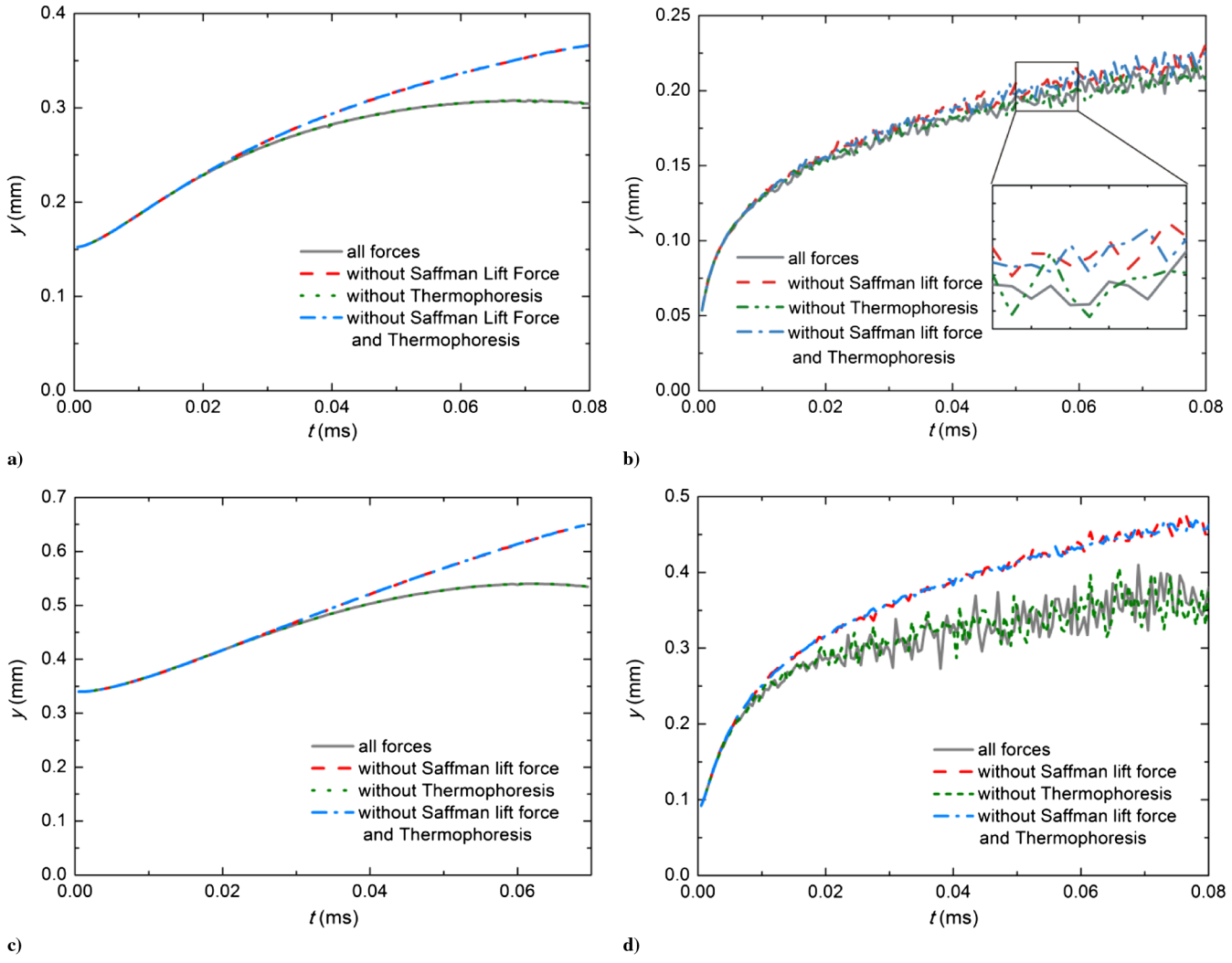

Fig. 4 *Y* position of particles with time on four force conditions.

Saffman lift force and thermophoresis. The conditions for cases of Figs. 4a–4d are a) $Ma_0 = 2.05$, $d_p = 1.0$ μm, b) $Ma_0 = 2.05$, $d_p = 0.05$ μm, c) $Ma_0 = 3.01$, $d_p = 1.0$ μm, and d) $Ma_0 = 3.01$, $d_p = 0.05$ μm, respectively. The oscillation in Figs. 4b and 4d is due to Brownian motion.

According to Fig. 4, the trajectory of the particle with all the four forces functioning superposes that of the particle with no thermophoresis, which means the thermophoretic force does not play an important role in this process. However, the particle without Saffman lift force on it moves along a different trajectory, and this trajectory is almost the same as the one without Saffman lift force and thermophoresis, which proves that the Saffman lift force plays an important role and the thermophoresis is a negligible factor. In addition, the Brownian motion of the particles with a diameter of 0.05 μm is much severer than that of the particles of 1.0 μm in diameter. And with larger Mach number of the main flow, the Brownian motion will become even severer.

An interesting phenomenon noticed in Fig. 4 is that the particles tend to move up away from the wall. The reason is illustrated in Fig. 5. It is well known that an induced shock wave emerges when a supersonic stream flows along a flat plate due to the existence of the boundary layer. The induced shock wave is an oblique shock, and when the flow moves across it, its velocity direction and magnitude change. The flow velocity in the y direction will no longer be zero, but above zero. Thus, in the presence of the drag force of the fluid, the particles will move away from the wall. Because the induced shock wave emerges at the leading edge of the wall, this effect is termed the "leading-edge lift effect on particles." A similar phenomenon occurs when the particle moves across an oblique shock wave generated by an inclined plate in a supersonic flowfield [18], thus the authenticity of the simulation.

Actually, this effect also emerges in low-speed flows, and it is also caused by the existence of the boundary layer. The difference is that there is no induced shock wave in low-speed flows. Further investigation is not included in our present work because the supersonic case is our main concern.

Another interesting phenomenon is that the particle trajectory with the Saffman lift force is lower than that without it, which indicates that one component of the Saffman force is in the negative y direction. The reason is that, when the particle runs into the boundary layer, its velocity is greater than that of the surrounding fluid, that is, the particle is leading the surrounding fluid, and so the Saffman lift force works toward the wall.

B. Effect of Initial Position

Particles enter the computational domain with the same velocity as that of the main flow, but in different y positions above the plate. In Fig. 5, we can see that the particles move across the induced shock wave, and then enter the boundary layer, but their experiences are not the same. For example, the particles closer to the wall encounter the shock wave and the boundary layer earlier, and the distance between the shock wave and the boundary layer is shorter. Besides, the Saffman lift force exerted on the particles varies due to the nonuniform distribution of the velocity in the boundary layer, which certainly affects the motion of the particles. To investigate the effect of the initial y position, the trajectories of the particles injected from different y positions are examined. The particles with an initial Mach number of 3.01 and a diameter of 0.5 μm are studied. The results are shown in Fig. 6.

Figure 6 shows that the higher the initial position y_0 is, the more likely the particle moves away from the wall. As y_0 decreases, the particle moves up first, and then moves down toward the wall. If y_0 is low enough, the particle will finally touch the wall. For example, when y_0 is 0.175 mm, the effect of the upward drag force overwhelms the effect of the downward Saffman lift force, resulting in an upward

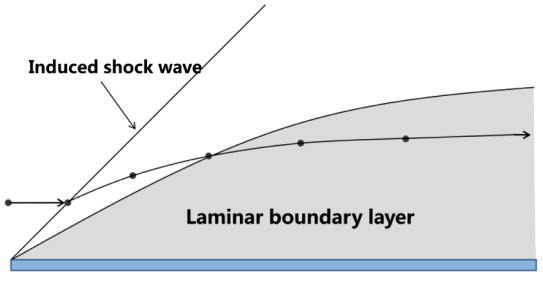

Fig. 5 Leading-edge lift effect of particles.

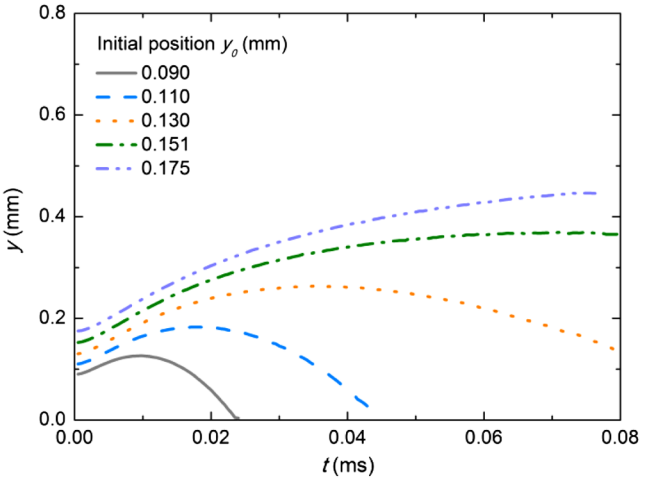

Fig. 6 Trajectories of particles injected from different initial y positions.

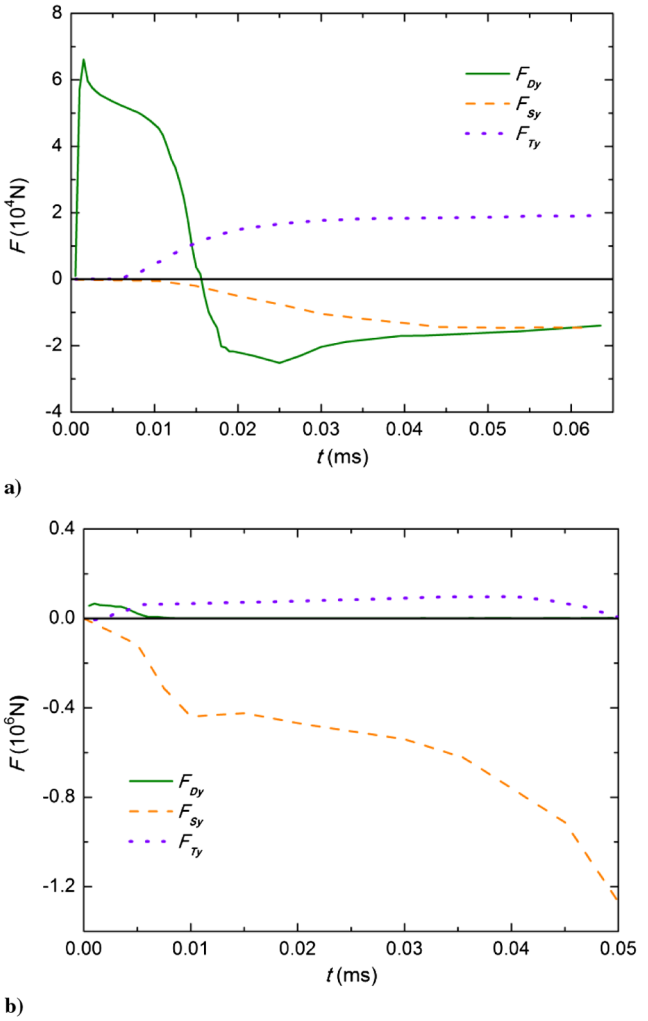

Fig. 7 Force analysis of two typical particle-motion patterns.

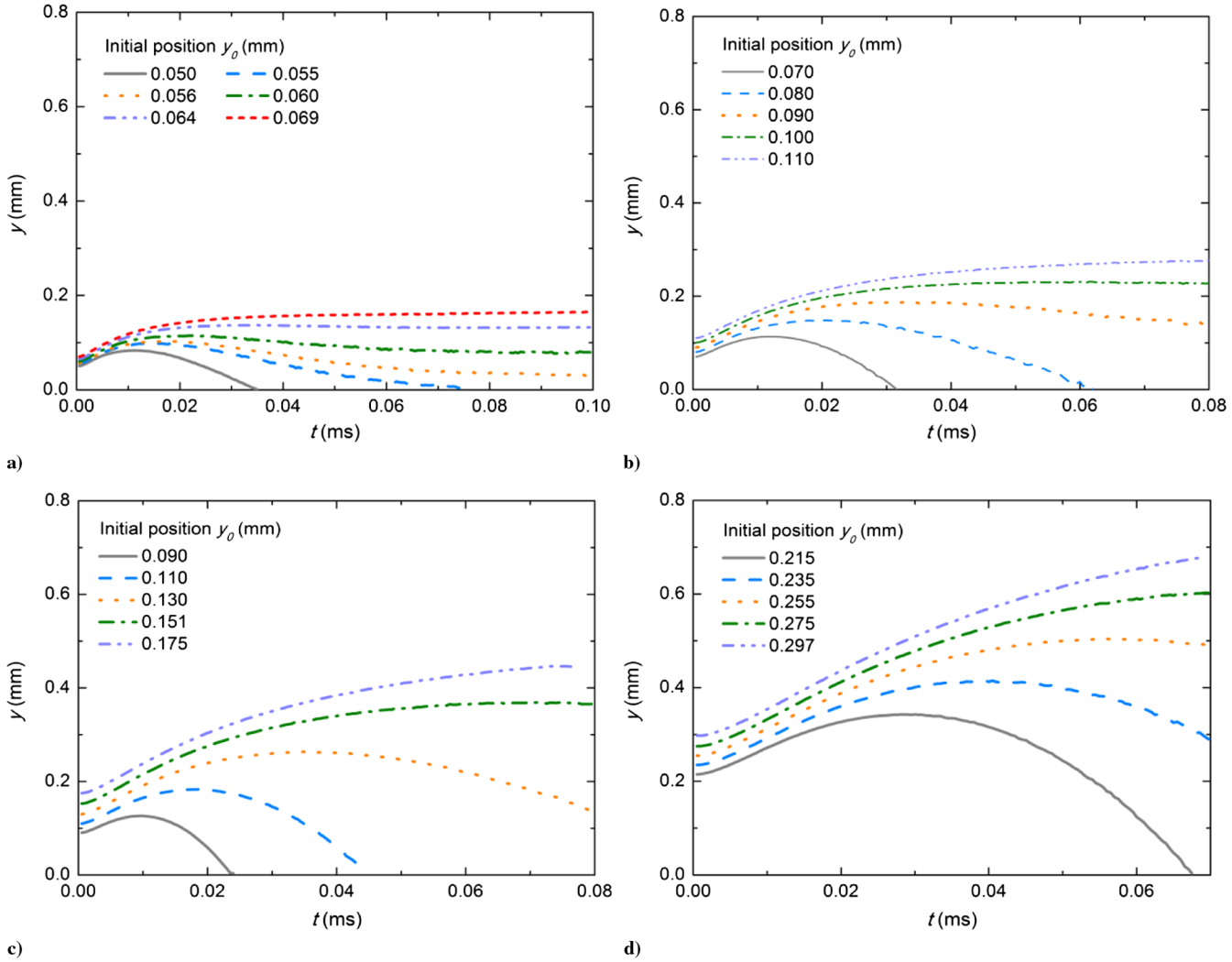

Fig. 8 Effect of initial Mach number.

motion of the particle. However, when y_0 is 0.09 mm, the Saffman lift force is great enough to force the particle to move downward and finally touch the wall. The reason lies in the relative magnitude of the drag force and the Saffman lift force, as shown in Fig. 7. The magnitude in Fig. 7 is the force on per kilogram particles. In the boundary layer, for the particle away from the wall, the upward drag force is greater compared with the Saffman lift force, and lasts longer. On the contrary, the particle closer to the wall experiences a greater Saffman lift force.

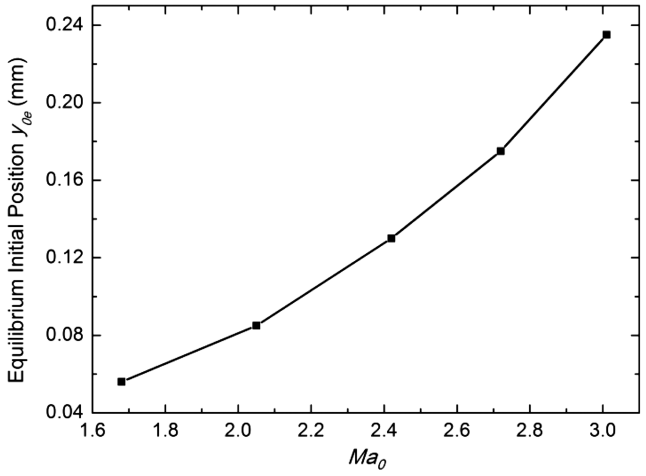

Fig. 9 Effect of Mach number on equilibrium initial position.

C. Effect of Initial Mach Number

According to the laws of aerodynamics, the intensity and direction of the induced shock wave vary as the initial flow Mach number changes. When the Mach number increases, the angle between the shock wave and the wall decreases (i.e., more oblique), which affects the drag force imposing on the particles. The Mach number of the main flow also has an effect on the structure of the boundary layer. The boundary layer is thinner and the velocity gradient is larger when the Mach number increases, which affects the Saffman lift force acting on the particles. The influences of the initial Mach number of the main flow are illustrated in Fig. 8. The particle diameter in Fig. 8 is 0.5 μm. And the initial Mach number in Figs. 8a–8d is 1.68, 2.05, 2.41, and 3.01, respectively. For the sake of a comprehensive analysis, the initial particle positions in each picture include those for moving upward and downward.

According to our results, when the initial Mach number of the main flow Ma_0 equals 1.68, there is an equilibrium initial position. The particle injected from this position finally moves along the stream, but the distance between the particle and the wall is zero. In Fig. 8a, the equilibrium initial position is between 0.055 and 0.056 mm, that is, the trajectory of the particle is between the dashed line and the dotted line. The reason why there exists an equilibrium position is also the interaction of the drag force and the Saffman lift force. As the particle moves across the induced shock wave, the drag force makes it move upward. When it enters the boundary layer, the greater Saffman lift force forces it to move downward to the wall. At the same time, the relative velocity between the particle and the fluid becomes smaller, which means both the drag force and the Saffman lift force are weakened (especially the Saffman lift force). Finally, the relative

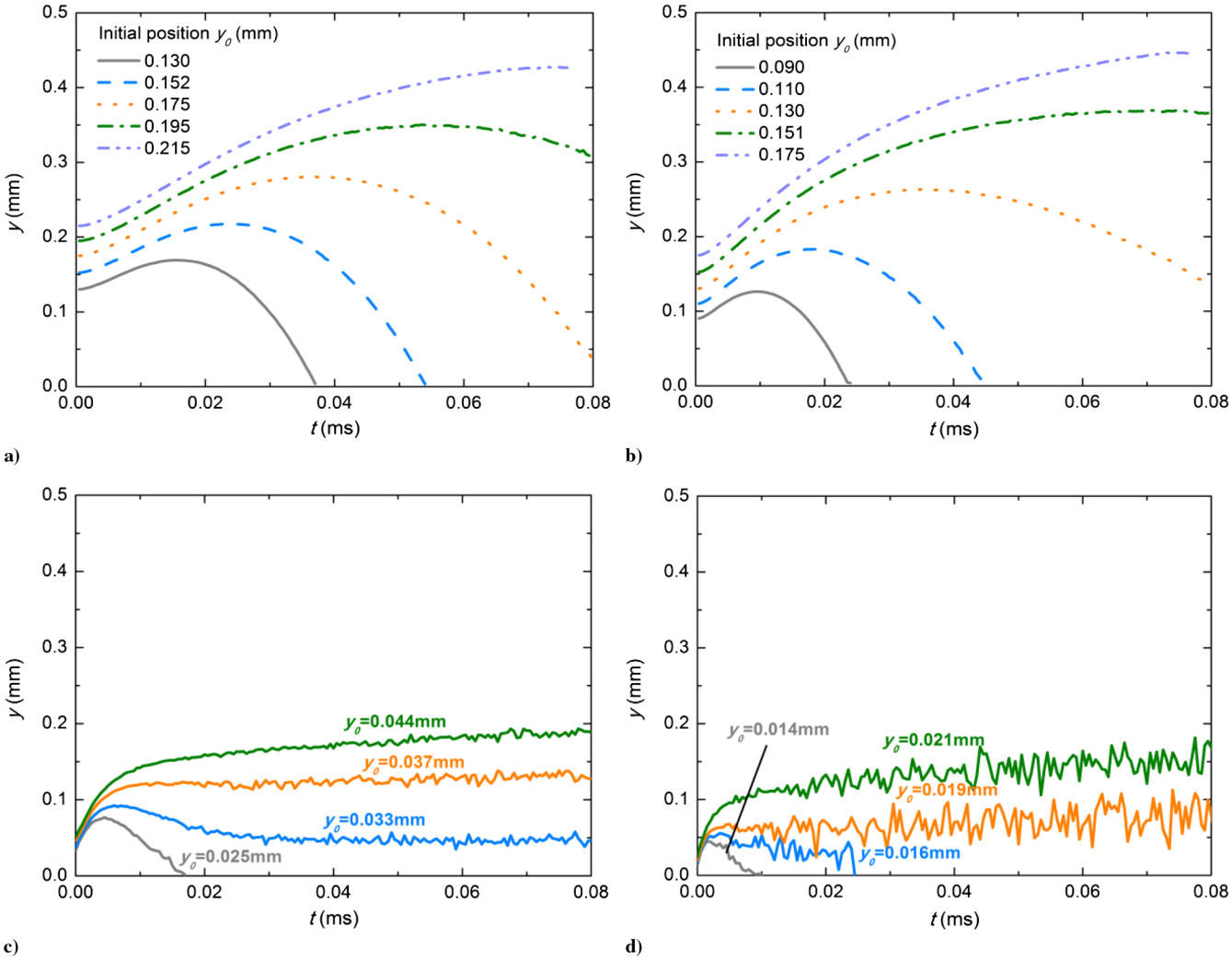

Fig. 10 Effect of particle size.

velocity becomes zero and the Saffman lift force disappears, and the particle moves along the stream. From Fig. 8a, we also discovered that the particles injected from above the equilibrium position finally move along the trajectories almost parallel to the wall. These particles never touch the wall unless the boundary layer turns into turbulent. But, the particles injected below the equilibrium initial position will touch the wall at last.

However, in Figs. 8b–8d, there is no obvious equilibrium initial position. Owing to the high velocity, the particles move across the outlet before they reach equilibrium of force, which means they are still accelerating or decelerating. They may reach equilibrium in the laminar boundary layer or enter the turbulent boundary layer before they reach equilibrium. Here, we assume that there exists an equilibrium initial position in all cases.

When comparing Figs. 8a–8d, we find that the equilibrium initial position becomes higher as the initial Mach number increases. Actually, as the Mach number increases, the velocity gradient in the boundary layer becomes larger, resulting in an increase of the Saffman lift force. Thus, the particle has to be injected from higher positions in order not to touch the wall. The variations of the equilibrium initial position caused by the Mach number are shown in Fig. 9.

D. Effect of Particle Size

According to the theory of particle dynamics, the drag force and the Saffman lift force on the particle vary as the particle size changes, because the flowfield around the particle changes. Under the condition of rarefied flowfield, the collision frequency of the fluid molecules with the particle decreases if the particle is smaller, and the Brownian motion is severe. The change of the collision frequency brings about the variation of the drag force, Saffman lift force, and Brownian force on the particle, resulting in different motion patterns of particles of different sizes. The effect of particle size is illustrated in Figs. 10 and 11. The initial Mach number in Fig. 10 is 2.41. And the particle diameter in Figs. 10a–10d is 1.0, 0.5, 0.1, and 0.05 μm, respectively. It is indicated that, as the particle diameter increases, the equilibrium position becomes higher. In other words, the particle tends to move toward the wall as its size increases. The reason is that,

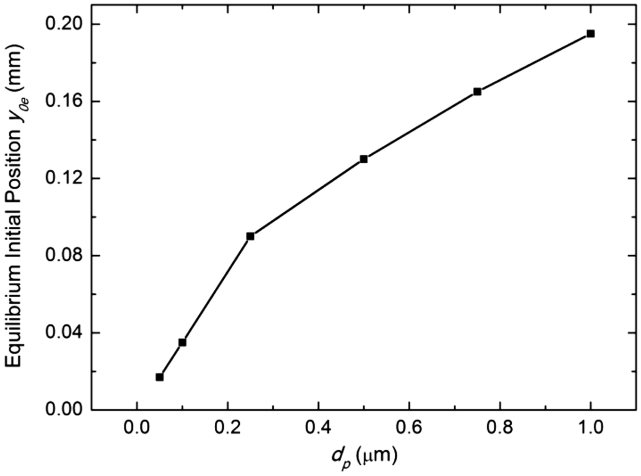

Fig. 11 Effect of particle size on equilibrium initial position.

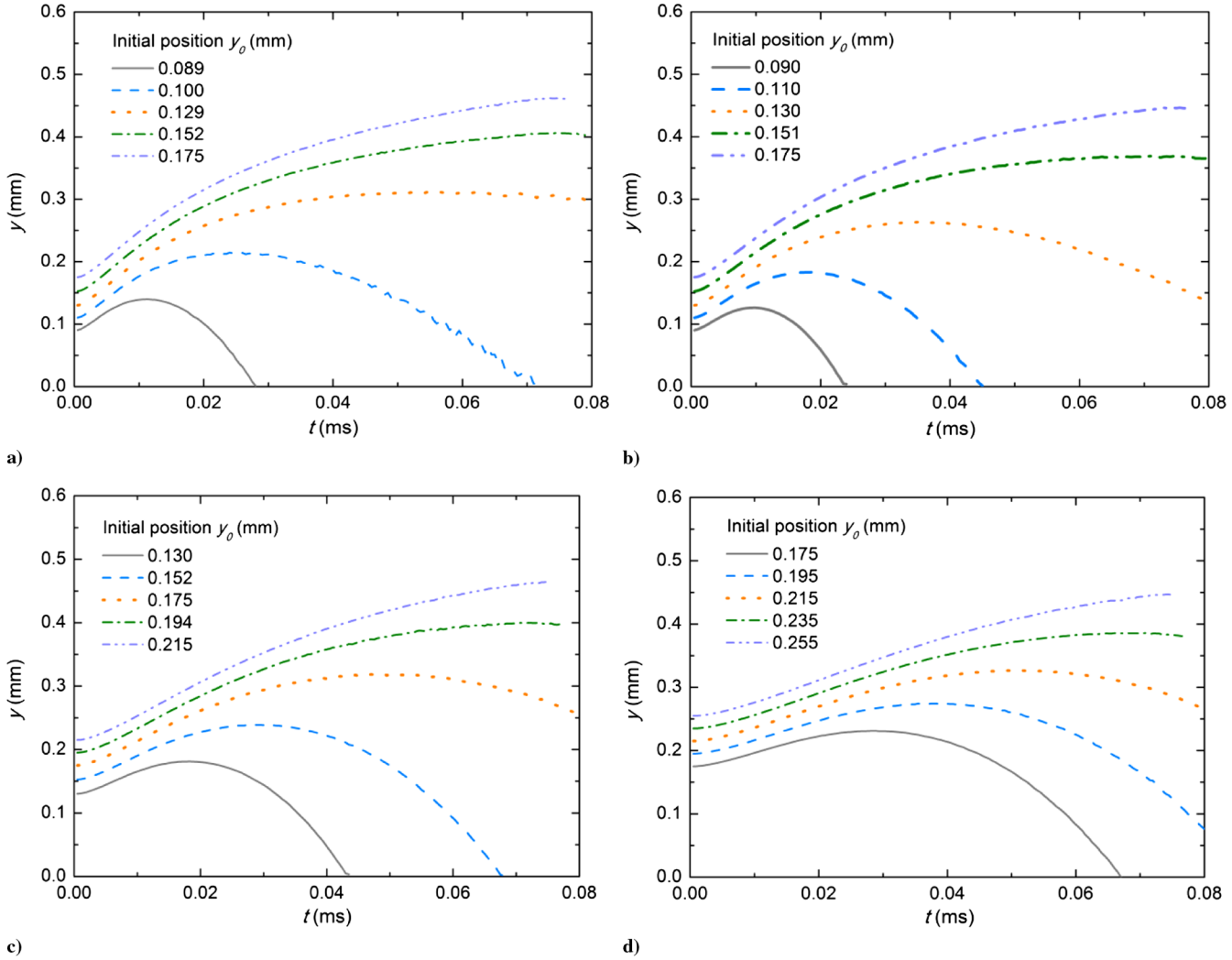

Fig. 12 Effect of particle density.

when the particle is larger, the Saffman lift force on it increases faster than the drag force. From the expressions of drag force and Saffman lift force, it follows that approximately $F_D \propto a$ and $F_S \propto a^2$, and so the Saffman lift force increases more rapidly as the particle size increases.

Another noticeable phenomenon is that the Brownian motion of smaller particles is severer. In Fig. 10c, the Brownian force on the particle is small and does not play a dominating role in the movement. However, in Fig. 10d, the Brownian motion is obvious and the particles injected close to the wall are very likely to touch the wall. Actually, in most cases in our research, the Brownian motion does not affect the macroscopic motion of the particles too much. Only when the particle is very small and very close to the wall, and the Mach number is large, the Brownian motion is important. Further investigation about the Brownian force is not included in the present work, for we are mainly concerned with the study of the macroscopic motion of the particles here.

E. Effect of Particle Density

The particle density also affects the particle motion. The denser the particle is, the slower it accelerates under the same net force. Besides water droplet, different particles are examined to discover the effect of density on the particle motion, including kerosene droplet (780 kg/m^3), carbon particle (2000 kg/m^3), and titanium dioxide particle (4000 kg/m^3). The initial Mach number in Fig. 12 is 2.41, and the particle diameter is 0.5 μm. The particle material in Figs. 12a–12d is kerosene, water, carbon, and titanium dioxide, respectively. The results in Figs. 12 and 13 show that, as the density of the particle increases, the equilibrium position is getting higher. In fact, as the density increases, the inertia of the particle increases, resulting in a longer reaction to the forces acting on it. As the drag force works for a shorter period than the Saffman lift force, the particle with higher density moves upward for a shorter distance.

VI. Discussion

From the preceding analysis and results, we conclude that the submicron-particle motion in a laminar supersonic boundary layer

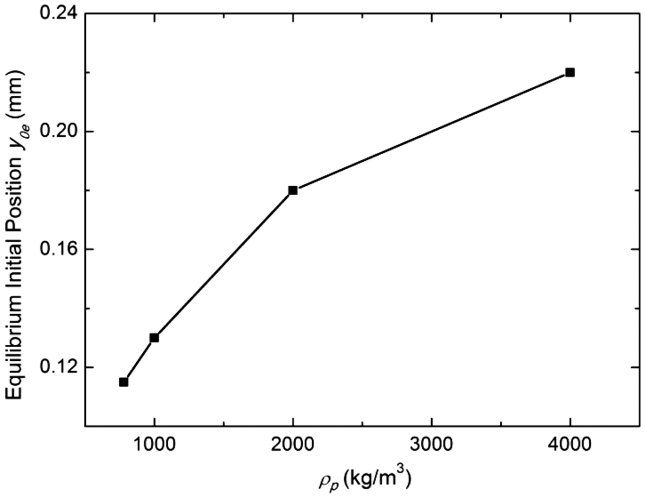

Fig. 13 Effect of particle density on equilibrium initial position.

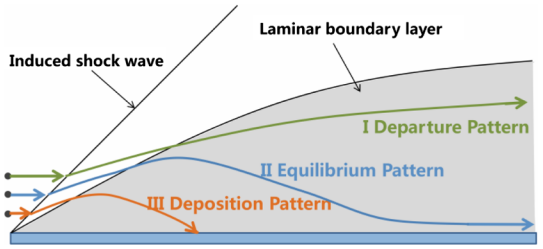

Fig. 14 Three particle-motion patterns.

above an adiabatic flat plate has three patterns (see Fig. 14): 1) the particle moves upward, finally moves almost along the stream and will not touch the wall (I); 2) the particle moves upward first, then downward, and finally moves almost along the stream, but it does not reach the wall (II); and 3) the particle moves upward first, and then downward until it reaches the wall (III).

To describe the three particle-motion patterns, a dimensionless number Φ is proposed. The main parameters determining the motion patterns include the initial velocity U_0, initial position y_0, particle diameter d_p, initial gas density ρ_{g0}, initial gas dynamic viscosity μ_{g0}, particle density ρ_p, initial mean free path of a gas molecule λ_0, and initial bulk modulus of gas E_{v0}. Φ can be expressed as

$$\Phi = f(V_0, \rho_{g0}, \mu_{g0}, E_v, \lambda_0, d_p, \rho_p, y_0) \tag{14}$$

The Buckingham method is applied to determine the form of Φ:

$$\Phi = F\left(Re_{p0}, Ma_0, Kn_0, \frac{y_0}{d_p}, \frac{\rho_{g0}}{\rho_p}\right) \tag{15}$$

in which $Re_{p0} = \rho_{g0} V_0 d_p / \mu_{g0}$ is the initial particle Reynolds number. Since $Kn_0 \propto Ma_0 / Re_{p0}$, the preceding form of Φ can be rewritten as

$$\Phi = \varphi\left(Re_{p0}, Ma_0, \frac{y_0}{d_p}, \frac{\rho_{g0}}{\rho_p}\right) \tag{16}$$

Actually, to determine the range of Φ for each particle-motion pattern, the range of Φ for pattern II has to be determined first. Once it is given, the range of Φ for patterns I and III can be inferred.

From Eq. (16), it can be inferred that the ratio of equilibrium initial position y_{0e} to the particle diameter (i.e., y_{0e}/d_p) is the function of Ma_0, Re_{p0}, and ρ_{g0}/ρ_p. Their relationships are given in Figs. 15a–15c, which show that the distributions have the form of power law. Thus, it is assumed that the formula has the form of Eq. (17). Then, a fitting formula [Eq. (18)] of these three factors is concluded.

$$\frac{y_{0e}}{d_p} = p Ma_0^{n_1} Re_{p0}^{n_2} \left(\frac{\rho_{g0}}{\rho_p}\right)^{n_3} + q \tag{17}$$

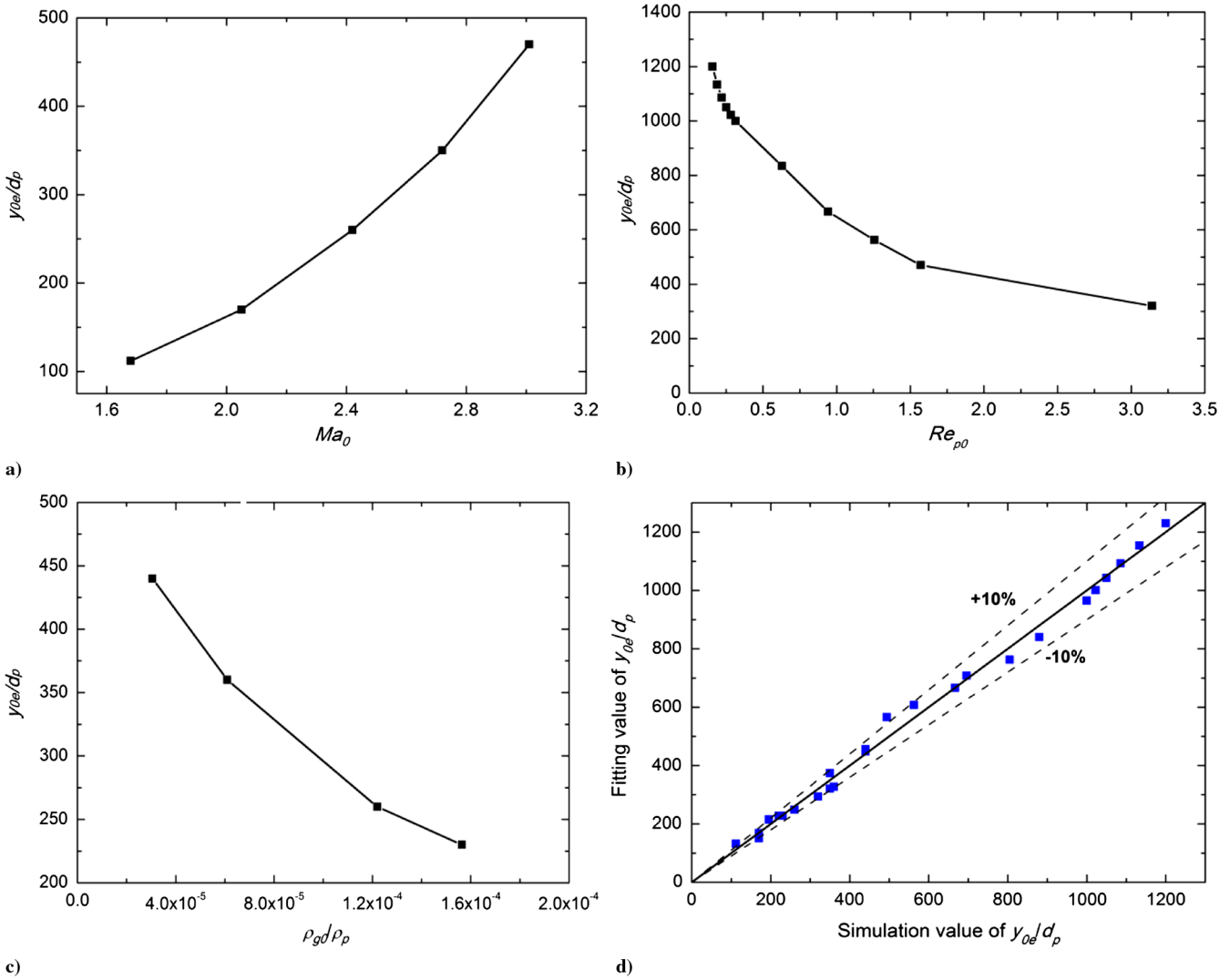

Fig. 15 The tendency of equilibrium initial position.

$$\frac{y_{0e}}{d_p} = 0.089 Ma_0^{2.416} Re_{p0}^{-0.388} \left(\frac{\rho_{g0}}{\rho_p}\right)^{-0.627} + 105.02 \qquad (18)$$

Figure 15d indicates the good performance of the fitting formula within the error of 10%. When both sides in Eq. (18) are divided by y_{0e}/d_p, and y_{0e} is replaced by y_0, we get

$$\Phi = \left(\frac{y_0}{d_p}\right)^{-1} \left[0.089 Ma_0^{2.416} Re_{p0}^{-0.388} \left(\frac{\rho_{g0}}{\rho_p}\right)^{-0.627} + 105.02\right] \qquad (19)$$

when $0.8 < \Phi < 1.2$ is for pattern II. Thus, when $\Phi < 0.8$ and $\Phi > 1.2$, particle-motion patterns I and III occur, respectively.

With the dimensionless number Φ, the motion patterns of a particle can be determined under different conditions, like different Mach number and different particle size. More important, Φ can be calculated with initial variables, which means it is predetermined before the particle moves across the induced shock wave.

VII. Conclusions

In this paper, a model has been developed to study the submicron-particle-motion patterns in a laminar supersonic boundary layer above a flat plate. The range of the particle diameter is from 0.05 to 1.0 μm, and the initial Mach number is from 1.68 to 3.01. Several types of particles, including water droplet (1000 kg/m^3), kerosene droplet (780 kg/m^3), carbon particle (2000 kg/m^3), and titanium dioxide particle (4000 kg/m^3), are examined. It is concluded that there are three particle-motion patterns when they enter the supersonic boundary layer, which are 1) departure pattern, 2) equilibrium pattern, and 3) deposition pattern. The drag force and the Saffman lift force play dominating roles in determining the movement patterns, and thermophoretic force and Brownian force are of less importance. The effects of initial position, Mach number, particle size, and particle density are investigated. The results show that the particle tends to move toward the wall as the initial Mach number, particle size, and particle density increase, and when the initial position is lower. A dimensionless number $\Phi = (y_0/d_p)^{-1}[0.089 Ma_0^{2.416} Re_{p0}^{-0.388} (\rho_{g0}/\rho_p)^{-0.627} + 105.02]$ has also been proposed to describe them. The particle moves in the patterns of I, II, and III when $\Phi < 0.8$, $0.8 < \Phi < 1.2$, and $\Phi > 1.2$, respectively.

Acknowledgment

This work was financially supported by the National Natural Science Foundation of China for Creative Research Groups under the contract number 51121092.

References

[1] Liu, G., Marshall, J. S., Li, S. Q., and Yao, Q., "Discrete-Element Method for Particle Capture by a Body in an Electrostatic Field," *International Journal for Numerical Methods in Engineering*, Vol. 84, No. 13, 2010, pp. 1589–1612. doi:10.1002/nme.v84.13

[2] Goren, S. L., "Thermophoresis of Aerosol Particles in the Laminar Boundary Layer on a Flat Plate," *Journal of Colloid and Interface Science*, Vol. 61, No. 1, 1977, pp. 77–85. doi:10.1016/0021-9797(77)90416-7

[3] Mills, A. F., Xu, H., and Ayazi, F., "The Effect of Wall Suction and Thermophoresis on Aerosol Particle Deposition from a Laminar Boundary Layer on a Flat Plate," *International Journal of Heat and Mass Transfer*, Vol. 27, No. 7, 1984, pp. 1110–1113. doi:10.1016/0017-9310(84)90127-3

[4] Epstein, M., Hauser, G. M., and Henry, R. E., "Thermophoretic Deposition of Particles in Natural Convection Flow from a Vertical Plate," *Journal of Heat Transfer*, Vol. 107, No. 2, 1985, pp. 272–276. doi:10.1115/1.3247410

[5] Gökog˘lu, S. A., and Rosner, D. E., "Viscous Dissipation Effects on Thermophoretically Augmented Aerosol Particle Transport Across Laminar Boundary Layers," *International Journal of Heat and Fluid Flow*, Vol. 6, No. 4, 1985, pp. 293–297. doi:10.1016/0142-727X(85)90066-9

[6] Gökog˘lu, S. A., and Rosner, D. E., "Thermophoretically Enhanced Mass Transport Rates to Solid and Transpiration-Cooled Walls Across Turbulent (Law-of-the-Wall) Boundary Layers," *Industrial & Engineering Chemistry Fundamentals*, Vol. 24, No. 2, 1985, pp. 208–214. doi:10.1021/i100018a013

[7] Gökoglu, S. A., and Rosner, D. E., "Thermophoretically Augmented Mass Transfer Rates to Solid Walls Across Laminar Boundary Layers," *AIAA Journal*, Vol. 24, No. 1, 1986, pp. 172–179. doi:10.2514/3.9239

[8] Garg, V. K., and Jayaraj, S., "Thermophoresis of Aerosol Particles in Laminar Flow over Inclined Plates," *International Journal of Heat and Mass Transfer*, Vol. 31, No. 4, 1988, pp. 875–890. doi:10.1016/0017-9310(88)90144-5

[9] Garg, V. K., and Jayaraj, S., "Thermophoretic Deposition in Crossflow over a Cylinder," *Journal of Thermophysics and Heat Transfer*, Vol. 4, No. 1, 1990, pp. 115–116. doi:10.2514/3.29164

[10] Chiou, M. C., and Cleaver, J. W., "Effect of Thermophoresis on Sub-Micron Particle Deposition from a Laminar Forced Convection Boundary Layer Flow onto an Isothermal Cylinder," *Journal of Aerosol Science*, Vol. 27, No. 8, 1996, pp. 1155–1167. doi:10.1016/0021-8502(96)00045-6

[11] Chiou, M. C., "Effect of Thermophoresis on Submicron Particle Deposition from a Forced Laminar Boundary Layer Flow onto an Isothermal Moving Plate," *Acta Mechanica*, Vol. 129, Nos. 3–4, 1998, pp. 219–229. doi:10.1007/BF01176747

[12] Chiou, M. C., "Particle Deposition from Natural Convection Boundary Layer Flow onto an Isothermal Vertical Cylinder," *Acta Mechanica*, Vol. 129, Nos. 3–4, 1998, pp. 163–176. doi:10.1007/BF01176743

[13] Chiou, M. C., "Submicron Particle Deposition from a Laminar Boundary-Layer Flow onto an Isothermal Vertical Solid Plate," *Acta Mechanica*, Vol. 143, Nos. 3–4, 2000, pp. 229–253. doi:10.1007/BF01170950

[14] Bagchi, P., and Balachandar, S., "Inertial and Viscous Forces on a Rigid Sphere in Straining Flows at Moderate Reynolds Numbers," *Journal of Fluid Mechanics*, Vol. 481, April 2003, pp. 105–148. doi:10.1017/S002211200300380X

[15] Ling, Y., Haselbacher, A., and Balachandar, S., "Importance of Unsteady Contributions to Force and Heating for Particles in Compressible Flows: Part 1: Modeling and Analysis for Shock–Particle Interaction," *International Journal of Multiphase Flow*, Vol. 37, No. 9, 2011, pp. 1026–1044. doi:10.1016/j.ijmultiphaseflow.2011.07.001

[16] Tedeschi, G., Gouin, H., and Elena, M., "Motion of Tracer Particles in Supersonic Flows," *Experiments in Fluids*, Vol. 26, No. 4, 1999, pp. 288–296. doi:10.1007/s003480050291

[17] Henderson, C. B., "Drag Coefficients of Spheres in Continuum and Rarefied Flows," *AIAA Journal*, Vol. 14, No. 6, 1976, pp. 707–708. doi:10.2514/3.61409

[18] Henderson, C. B., "Reply by Author to M. J. Walsh," *AIAA Journal*, Vol. 15, No. 6, 1977, pp. 894–895. doi:10.2514/3.60724

[19] Talbot, L., Cheng, R. K., Schefer, R. W., and Willis, D. R., "Thermophoresis of Particles in a Heated Boundary Layer," *Journal of Fluid Mechanics*, Vol. 101, No. 4, 1980, pp. 737–758. doi:10.1017/S0022112080001905

[20] Sone, Y., and Aoki, K., "A Similarity Solution of the Linearized Boltzmann Equation with Application to Thermophoresis of a Spherical Particle," *Journal de Mécanique Théorique et Appliquée*, Vol. 2, No. 1, 1983, pp. 3–12.

[21] Yamamoto, K., and Ishihara, Y., "Thermophoresis of a Spherical Particle in a Rarefied Gas of a Transition Regime," *Physics of Fluids*, Vol. 31, No. 12, 1988, pp. 3618–3624. doi:10.1063/1.866878

[22] Loyalka, S. K., "Thermophoretic Force on a Single Particle—I. Numerical Solution of the Linearized Boltzmann Equation," *Journal of Aerosol Science*, Vol. 23, No. 3, 1992, pp. 291–300. doi:10.1016/0021-8502(92)90329-T

[23] Takata, S., Aoki, K., and Sone, Y., "Thermophoresis of a Sphere with a Uniform Temperature: Numerical Analysis of the Boltzmann Equation for Hard-Sphere Molecules," *Rarefied Gas Dynamics: Theory and Simulations*, edited by Weaver, D., Vol. 159, Progress in Astronautics and Aeronautics, AIAA, Washington, D.C., 1994, pp. 626–639.

[24] Dandy, D. S., and Dwyer, H. A., "A Sphere in Shear Flow at Finite Reynolds Number: Effect of Shear on Particle Lift, Drag, and Heat

Transfer," *Journal of Fluid Mechanics*, Vol. 216, July 1990, pp. 381–410.
doi:10.1017/S0022112090000477

[25] McLaughlin, J. B., "The Lift on a Small Sphere in Wall-Bounded Linear Shear Flows," *Journal of Fluid Mechanics*, Vol. 246, Jan. 1993, pp. 249–249.
doi:10.1017/S0022112093000114

[26] Mei, R., "An Approximate Expression for the Shear Lift Force on a Spherical Particle at Finite Reynolds Number," *International Journal of Multiphase Flow*, Vol. 18, No. 1, 1992, pp. 145–147.
doi:10.1016/0301-9322(92)90012-6

[27] Kurose, R., and Komori, S., "Drag and Lift Forces on a Rotating Sphere in a Linear Shear Flow," *Journal of Fluid Mechanics*, Vol. 384, No. 4, 1999, pp. 183–206.
doi:10.1017/S0022112099004164

[28] Bagchi, P., and Balachandar, S., "Effect of Free Rotation on the Motion of a Solid Sphere in Linear Shear Flow at Moderate Re," *Physics of Fluids*, Vol. 14, No. 8, 2002, pp. 2719–2737.
doi:10.1063/1.1487378

[29] Li, A., and Ahmadi, G., "Dispersion and Deposition of Spherical Particles from Point Sources in a Turbulent Channel Flow," *Aerosol Science and Technology*, Vol. 16, No. 4, 1992, pp. 209–226.
doi:10.1080/02786829208959550

[30] Uhlenbeck, G. E., and Ornstein, L. S., "On the Theory of the Brownian Motion," *Physical Review*, Vol. 36, No. 5, 1930, pp. 823–841.
doi:10.1103/PhysRev.36.823

[31] Crocco, L., "Sullo Strato Limite Laminare nei Gas Lungo una Lamina Plana," *Rendiconti Di Matematica e Delle Sue Applicazioni, V. Serie*, Vol. 5, No. 21, 1941, pp. 138–152.

R. Lucht
Associate Editor